

Two Decades of the Atlantic Meridional Overturning Circulation: Anatomy, Variations, Extremes, Prediction, and Overcoming Its Limitations

CARL WUNSCH AND PATRICK HEIMBACH

Department of Earth, Atmospheric and Planetary Sciences, Massachusetts Institute of Technology, Cambridge, Massachusetts

(Manuscript received 25 July 2012, in final form 9 March 2013)

ABSTRACT

The zonally integrated meridional volume transport in the North Atlantic [Atlantic meridional overturning circulation (AMOC)] is described in a 19-yr-long ocean-state estimate, one consistent with a diverse global dataset. Apart from a weak increasing trend at high northern latitudes, the AMOC appears statistically stable over the last 19 yr with fluctuations indistinguishable from those of a stationary Gaussian stochastic process. This characterization makes it possible to study (using highly developed tools) extreme values, predictability, and the statistical significance of apparent trends. Gaussian behavior is consistent with the central limit theorem for a process arising from numerous independent disturbances. In this case, generators include internal instabilities, changes in wind and buoyancy forcing fields, boundary waves, the Gulf Stream and deep western boundary current transports, the interior fraction in Sverdrup balance, and all similar phenomena arriving as summation effects from long distances and times. As a zonal integral through the sum of the large variety of physical processes in the three-dimensional ocean circulation, understanding of the AMOC, if it is of central climate importance, requires breaking it down into its unintegrated components over the entire basin.

1. Introduction

The oceanic meridional overturning circulation (MOC), a measure of the zonally integrated poleward-bound mass transport, has become emblematic of ocean circulation and its role in climate change [e.g., Solomon et al. (2007); the Intergovernmental Panel on Climate Change (IPCC) report]. Its value in the North Atlantic Ocean, in particular [Atlantic meridional overturning circulation (AMOC)], has been the subject of thousands of papers concerning its value today, in long intervals of past climate and its future magnitudes.¹ The present paper is not intended as a review of this now amorphous subject [see, e.g., Lozier (2012) for a summary discussion of the literature on the present circulation]. The purposes here are to 1) describe the present-day AMOC time-average properties over the entire Atlantic—insofar as

they can be determined—and their corresponding variability, 2) break its properties down into the elements generally suppressed in the integration process, 3) determine its resulting (linear) predictability, 4) examine the frequency of extreme events, and 5) suggest its usefulness is very limited. For the understanding of influence of the ocean on climate, much more informative measures of the circulation are required.

Discussions of the oceans in climate have usually assumed it to be operating in a very simple form, and the desire for simplicity is understandable. Such assumptions included the extended period when the ocean was represented as a swamp in climate models, acting as a simple storehouse of heat and freshwater. A step forward was taken by representing the ocean as a one-dimensional (in the vertical) system in steady state, commonly using either stacked boxes or one-dimensional “abyssal recipe” balances:

$$w \frac{dC}{dz} - K \frac{d^2C}{dz^2} = q, \quad (1)$$

where w and K are a velocity and a mixing coefficient and q is any source or sink for property C . These ideas have had a long run in the literature.

¹ The Citation Index reports over 2500 papers discussing the MOC or the Atlantic “thermohaline circulation.”

Corresponding author address: Carl Wunsch, Department of Earth, Atmospheric and Planetary Sciences, Massachusetts Institute of Technology, Cambridge, MA 02139.
E-mail: cwunsch@mit.edu

Once it became impossible to disregard the quantifiable lateral transports and redistributions of these properties, and of others such as carbon and nutrients, theoreticians and modelers moved on to assuming that the ocean was fundamentally two-dimensional (Southern Ocean studies sometimes being exceptions). Numerical models were constructed (e.g., Wright and Stocker 1991; Petoukhov et al. 2000) in meridional y and vertical z coordinates and sometimes coupled to overlying atmospheres.

Even when three-space-dimensional ocean models finally emerged, the zonally integrated properties of the circulation were retained as the sine qua non of the ocean circulation in climate. The volume of numbers required and the complexity of the zonally integrated fields are much less than that of the underlying three-dimensional ones, and it is an important part of science to seek out the essential and simplest elements describing any phenomenon. One can infer, however, that the community has clung to the MOC measure for so long at least in part as a consequence of the hugely popular conveyor belt or ribbon pictures of the circulation—pictures that are appealingly simple, easy to remember, and seemingly consistent with the attractive notion of the ocean as a convectively driven heat engine and that give the North Atlantic Ocean the starring role. At least two Hollywood films and now countless popularizations, textbooks, and even research papers have adopted the MOC cartoon as the essence of physical oceanography.

Although little observational evidence exists for its direct influence on the climate system, significant resources have been and are continuing to be devoted to field programs intended to provide direct measures of AMOC strength (e.g., Send et al. 2011; Rayner et al. 2011). Because such records are regional, and they at best increase in duration by 1 yr yr^{-1} , interpretation of the significance of inevitable temporal fluctuations can only be done with some understanding of ocean variability on longer time scales and on a global basis.

Here, we take advantage of the Estimating the Circulation & Climate of the Ocean (ECCO) climate state estimates (Wunsch and Heimbach 2013) and for which an earlier discussion (Wunsch and Heimbach 2007) is extended. This new estimate lengthens the estimation interval, includes full Arctic Sea coverage, has a much more complete sea ice model, and has improved vertical and meridional resolution among other changes described briefly below. Both previous and present estimates begin in 1992 with the advent of the World Ocean Circulation Experiment (WOCE)-era altimetry, hydrography, and other quasi-global datasets.

Readers will recognize that 19 yr is a minute interval relative to the known and inferred time scales of oceanic

and climate change. Only in that interval does the ocean become even marginally adequately observed. Models can be both quantitatively tested and constrained to a high degree of realism. In contrast, inferences on longer time scales are derived from extremely fragmentary data at best or are pure model extrapolations at worst and whose skill generally remains indeterminate. No inferences will be made here about oceanic behavior beyond the 2-decade time span of the relatively well-observed ocean. Deductions concerning, for example, the behavior of the AMOC 100 yr in the past or future are interesting and perhaps even useful but remain speculative in a way that will not be addressed.

2. The estimate

A number of discussions exist of the ECCO approach to state estimation. A summary for present purposes is that it is done by least squares fitting of a modern GCM [an evolved form of Adcroft et al. (2004)] including submodels representing vertical (Gaspar et al. 1990) and along-isopycnal (Redi 1982) mixing, parameterization of geostrophic eddies (Gent and McWilliams 1990), and a dynamic/thermodynamic sea ice component (Menemenlis et al. 2005; Losch et al. 2010; Heimbach et al. 2010). The model uses a nonlinear free surface with freshwater flux boundary conditions (Campin et al. 2004). It has rescaled height coordinates (Adcroft and Campin 2004) with 50 vertical levels and partial cell representation of bottom topography (Adcroft et al. 1997). A priori forcing fields are from the European Centre for Medium-Range Weather Forecasts (ECMWF) Interim Re-Analysis (ERA-Interim; Dee et al. 2011). The resulting constrained least squares problem is solved by the method of Lagrange multipliers through iterative improvement relying upon a quasi-Newton gradient search (Gilbert and Lemaréchal 1989). Each of the several billion data points (see Table 1) in the time interval of 19 yr (as of this writing) beginning in 1992 is weighted by a best-available estimate of its error variance. In contrast to previous such estimates, the objective or misfit function now explicitly separates required large-spatial-scale observations from those represented only as point values. See Wunsch and Heimbach (2013) for a discussion of the complete estimation system. Results in this paper are based on an early solution of what we refer to as ECCO-Production [ECCO-Global Ocean Data Assimilation Experiment (GODAE) follow on], version 4 in revision 2 and iteration 5 (ECCO-Production ver4.rev2.iter5).

In physical terms, the great majority of the volume of the ocean is, when averaged over days and tens of kilometers, in a state of low Rossby and Ekman numbers.

Thus, the dominating physics in the model and in the real ocean is that of geostrophic hydrostatic balance, with higher-order physics confined to comparatively very small regions. As one indicator, the correlation coefficient, giving all model depths equal weight between the numerically determined zonal density gradient $g\partial\rho/\partial x$ and the vertical shear $f\partial v/\partial z$, at 30°N between about 220 and 3000 m is 0.98. (If carried to the sea surface, the correlation falls to about 0.44.) Large-scale errors in the results are most likely to arise from small, but systematic, offsets between the model and the data, with those in turn sometimes resulting from the inability of boundary current systems to carry realistic property transports.

3. The Atlantic meridional overturning circulation

Let $V(\lambda, z, \phi, t)$ be the meridional volume (mass) transport as a function of longitude λ , depth z , latitude ϕ , and time t and where monthly-mean values are being used. Values are calculated from the estimated state for each model level for each 1° of longitudinal distance. Denote the complete zonal integral from coast to coast as

$$V_{cc}(z, \phi, t) = \sum_j V(\lambda_j, z, \phi, t), \quad (2)$$

where the λ_j are on a uniform 1° separation. Figure 1 displays the time-average zonally integrated meridional transport as a function of latitude ϕ and depth z , $\bar{V}_{cc}(z, \phi)$ per meter of depth, and Fig. 2 shows transport plotted as an accumulating vertical profile from the free surface $\eta(t)$ at six representative latitudes. Following Wunsch (2012), the AMOC is defined as the maximum transport

$$V_{\text{MOC}}[z_{\text{max}}(t), \phi, t] = \max_z \left[\int_{z(\phi, t)}^{\eta(\phi, t)} V_{cc}(z, \phi, t) dz \right], \quad (3)$$

where the maximizing depth is itself a function of time. Values of $V_{\text{MOC}}[z_{\text{max}}(t), \phi, t]$ and of $z_{\text{max}}(\phi, t)$ are readily determined. Their 19-yr time-mean $\bar{V}_{\text{MOC}}[\bar{z}_{\text{max}}(\phi), \phi]$ and $\bar{z}_{\text{max}}(\phi)$ are displayed in Fig. 3, along with the standard errors from the monthly-mean estimates. The term $\bar{V}_{\text{MOC}}[\bar{z}_{\text{max}}(\phi), \phi]$ shows a slow increase from about 14 Sv (1 Sv $\equiv 10^6 \text{ m}^3 \text{ s}^{-1}$) at 30°S to 16 Sv at about 15°N, then declining to about 10 and 2 Sv near 50° and 65°N, respectively, necessarily vanishing at the pole. Accounting for the meridional correlations in the error estimates is not difficult, but it has not been thought worthwhile at this present stage. In similar fashion, the

maximizing time-mean depth gradually shoals from about 1200 m in the far south to near 800 m in the far north. It lies at about 1000 m over a large latitude range in the northern subtropics. Large temporal variations at low latitudes are consistent with the expected short adjustment time scales there.

The calculation of V_{MOC} is carried to 70°N only. Beyond that latitude, the definition of a basinwide zonal integral becomes ambiguous as it would require inclusion of the interior Arctic Basin. The estimate is, however, consistent with the global results, which include the full Arctic region.

To summarize the results, $\bar{V}_{\text{MOC}}[z_{\text{max}}(t), \phi_j, t]$ at $\phi_j = 25^\circ\text{S}, 10^\circ\text{N}, 25^\circ\text{N}, 45^\circ\text{N},$ and 55°N , are displayed in Figs. 4 and 5, the latter showing the result when a mean seasonal cycle and its overtones are removed. The 10°N is representative of low latitudes and 45° and 55°N are indicative of the subpolar gyre with its longer time scales. The slightly redundant line at 16°N is sometimes included to facilitate comparison with the mooring data available on the western side of that line [Send et al. (2011), but not discussed here].

The emphasis in this paper is on the need to understand the flow and variability throughout the entire Atlantic Ocean; specific regional discussions are omitted. Nonetheless, note that the Rapid Climate Change (RAPID) array (Rayner et al. 2011) uniquely spans the North Atlantic at 26.5°N and provides a convenient partially independent test.² At that latitude, the Gulf Stream (Florida Current) is confined between the Florida and Bahama landmasses and with the independent measurements of the Florida Current transport (Meinen et al. 2010) it provides a convenient, if dynamically unusual, latitude for measurements (Kanzow et al. 2009). It is dynamically unusual because the Bahama Bank physically separates the continental boundary of the western boundary current from that relevant to the oceanic interior—a double western boundary—in a situation not encountered anywhere else in the Atlantic. Figure 6 provides a basis for a visual comparison with the RAPID result [see Baehr (2010)]. The 2010 drop in transport in the RAPID result (McCarthy et al. 2012) is conspicuous also in the ECCO estimate, albeit with a somewhat reduced amplitude. A shorter-lived reduction of similar magnitude appears to have occurred in 1998, and the longer state estimate shows that the particular event is not unusual.

At 25°N, the variance of the annual cycle in the state estimate is about 2.5 Sv². When removed (along with its

² Although the mooring data were withheld from the ECCO estimate, published mooring results use essentially the same wind field that is part of the state estimate prior.

TABLE 1. Data used in the ECCO decadal global 1°-resolution state estimates. Such tables are never completely up to date as new data are obtained. In the observation (Obs) column, MDT is mean dynamic topography, SLA is sea level anomaly, SSS is sea surface salinity, and SIC refers to sea ice cover. Temperature and salinity are T and S , respectively.

Obs	Instrument	Product/source	Area	Period	Interval
MDT	Gravity Recovery and Climate Experiment (GRACE) U. Texas-GRACE version 3 (GRACE3) Earth Gravitational Model 2008 (EGM2008)/Danish National Space Center (DNSC07) Ocean Topography Experiment (TOPEX)/Poseidon	Collecte Localisation Satellites (CLS)/German Research Centre for Geosciences (GFZ) National Geospatial-Intelligence Agency National Oceanic and Atmospheric Administration (NOAA)/Radar Altimeter Database System (RAD5) and Physical Oceanography Distributed Active Archive Center (PO.DAAC) NOAA/RADS and PO.DAAC NOAA/RADS and PO.DAAC	Global Global 65°N/S	— — 1993–2002	— — Daily
SLA	<i>Jason-1, Jason-2</i> <i>European Remote Sensing Satellite-1/2</i> <i>(ERS-1/2), Envisat</i> <i>Geosat Follow-On (GFO)</i> Blended, Advanced Very High Resolution Radiometer (AVHRR) (O/I) Tropical Rainfall Measuring Mission (TRMM) Microwave Imager (TMI) Advanced Microwave Scanning Radiometer for Earth Observing System (EOS) (AMSR-E)/Moderate Resolution Imaging Spectroradiometer (MODIS)/ <i>Aqua</i>	NOAA/RADS and PO.DAAC NOAA/RADS and PO.DAAC Group for High Resolution SST (GHRSSST) GHRSSST	65°N/S 82°N/S 65°N/S Global 40°N/S Global	2002–11 1992–2011 2001–08 1992–2011 1998–2004 2001–11	Daily Daily Daily Monthly Daily Daily
SSS	Various in situ Various in situ floats and sections. Argo, Profiling autonomous Lagrangian circulation explorer (PALACE) Expendable bathythermograph (XBT) Conductivity–temperature–depth (CTD) Southern Elephant Seals as Oceanographic Samplers (SEaOS)	<i>World Ocean Atlas 2009 (WOA09)</i> surface French Research Institute for Exploitation of the Sea (Ifremer) National Centers for Environmental Prediction (NCEP) Various Sea Mammal Research Unit (SMRU) and British Antarctic Survey (BAS) Pacific Marine Environmental Laboratory (PMEL)/NOAA	Global Global Global Sections Southern Ocean (SO) Tropics	Climatology 1992–2011 1992–2011 1992–2011 2004–10 1992–2011	Monthly Daily Daily Daily Daily
Mooring arrays	Tropical Ocean and Global Atmosphere (TOGA)/Tropical Atmosphere Ocean (TAO), Prediction and Research Moored Array in the Tropical Atlantic (PIRATA) Florida Straits	NOAA/Atlantic Oceanographic and Meteorological Laboratory (AOML) <i>WOA09</i> Forget (2010) National Snow and Ice Data Center (NSIDC)-0079 (Boostrap) NSIDC-0051 (NASA Team)	North Atlantic Global Global Arctic, SO Arctic, SO	1992–2011 1950–2008 1950–2002 1992–2011 1992–2011	Daily Mean Mean Daily Daily
T, S	Climatological. <i>WOA09</i> <i>Ocean Comprehensible Atlas (OCCA)</i>				
SIC	Satellite brightness temperature (passive microwave)				

TABLE 1. (Continued)

Obs	Instrument	Product/source	Area	Period	Interval
Wind stress	QuickSCAT	NASA Scatterometer Climatology of Ocean Winds (SCOW) (Risien and Chelton 2008)	Global Global	1999–2009 Climatology	Daily Monthly
SSH	Tide gauges	National Data Buoy Center (NBDC)/NOAA	Sparse Global	1992–2006 1992–2011	Monthly 2–14 day
Flux constraints	ERA-Interim, Japanese 25-year Reanalysis Project (JRA-25), NCEP, Common Ocean-Ice Reference Experiments (CORE) 2 variances	Various			
Balance constraints	—	—	Global	1992–2011	Mean
Bathymetry	—	Smith and Sandwell (1997), 5-minute Earth Topography (ETOPO5)	Global	—	—

first three overtones), the residual is quite noisy (Fig. 6) with a variance of 4.2 Sv^2 . If reduced to annual averages, the variance is about 1.1 Sv^2 . This present estimate does not resolve the mesoscale eddy field—which dominates oceanic kinetic energy and thus all of these variances are expected to be lower bounds on the true variability—and also dominates the moored velocity and temperature measurements. Fortunately, because geostrophic volume calculations from moored temperature (and assumed associated salinities) depend only upon differences at the ends of sections, it is characteristic of them that regional volume transports are insensitive to unresolved hydrodynamic structures, apart from eddies only partially sampled at the end points.

Calculations taken from coast to coast tend to strongly suppress noise from partially observed eddy fields. In contrast, partial sums, as in the Kanzow et al. (2008) and Send et al. (2011) array at 16°N , are much freer to vary, and one expects larger fluctuations relative to the mean to be seen in any volume transport integral extending partway across the ocean. In particular, any eddy extending fractionally across the partial section can produce net transports of many tens of Sverdrups and consequent potential sampling aliases, even when averaged over months. Thus, any detailed agreement between moored array results and those obtained here would be fortuitous. Trends in section fragments, even should they prove statistically significant, have no easy interpretation for the ocean as a whole, which will continue to follow overall mass and other conservation constraints.

When using moored data, other problems lie with the poorly measured near-continental margin regions and, in the abyss, the last from the impossibility of geostrophic transport calculations across topographic features.

The calculation of advected properties such as temperature, salt, or carbon does require the covariances of velocity with that property, and these are not always available in mooring data. Heat and other transports as computed from the state estimate will be discussed elsewhere.

That a climate model reproduces the observed AMOC can be regarded as a necessary but insufficient test; nonetheless, see the very wide range of nominal present-day values in the models employed by the IPCC Fourth Assessment. With the exception of the present subpolar 45° and 55°N results, the annual averages do not show any visual transport trends except over fractions of the record duration.

4. Spectral character

Figure 7 shows the estimated spectral densities at five latitudes, both with the annual cycle and its harmonics

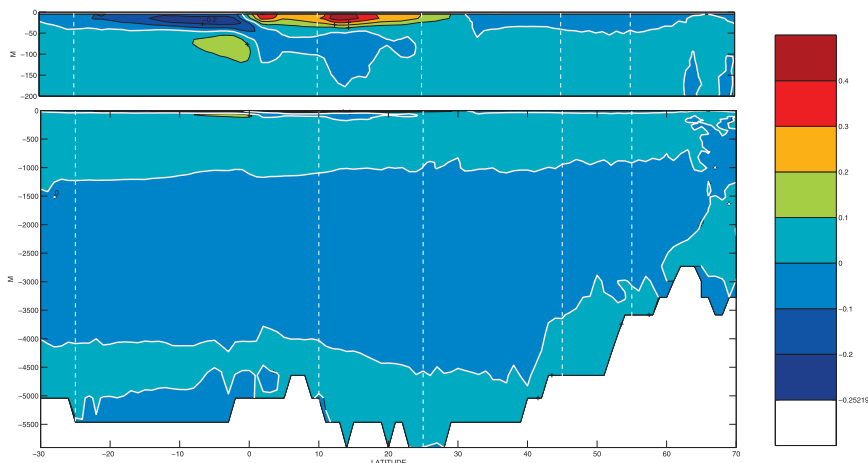


FIG. 1. A 19-yr avg of the estimated meridional transport V_{cc} per meter [$\text{Sv (m depth from ECCO-Production ver4)}^{-1}$]. The top 200 m are shown on an expanded scale. The white contour is the zero line. Vertical dashed lines are the positions used to display the temporal variability of V_{MOC} . Although the plot stops at 70°N , the estimate is carried to the pole, but it becomes impossible to define a simple transoceanic integral at the very highest latitudes. Five reference latitudes are shown as dashed lines. Negative latitudes are south of the equator.

and with them removed. Much of the tropical and subtropical annual cycle arises from the direct near-surface wind forcing (Jayne and Marotzke 2001). The residual spectrum has a weakly red character, unsurprising in a system with long memory capable of integrating effects over many decades and longer. The corresponding autocorrelations are also shown in Fig. 7 and are similarly characterized as being not far from a white-noise process, having a bit of memory out to about 3 months; the implications for predictability are discussed in the next section. The 45° and 55°N behavior has a more extended serial correlation, consistent with greater low-frequency energy. Histograms, showing a roughly Gaussian behavior, are in Fig. 8. A χ^2 test accepts the

null hypothesis of a Gaussian distribution at 95% confidence.

Estimates of the coherence among four pairs of six latitudes, computed to their nearest neighbor, are shown in Fig. 9. At periods longer than a few months, the most significant coherence is between 10° and 16°N (not shown) at zero phase. Transequatorial and subtropical to subpolar gyre, low-frequency coherences are weak (accounting for less than 25% of the low-frequency variance). Significant coherence exists between subpolar and subtropical latitudes lying in periods between about 5 and 2 months, but 180° out of phase, and strong evidence exists that this phase is

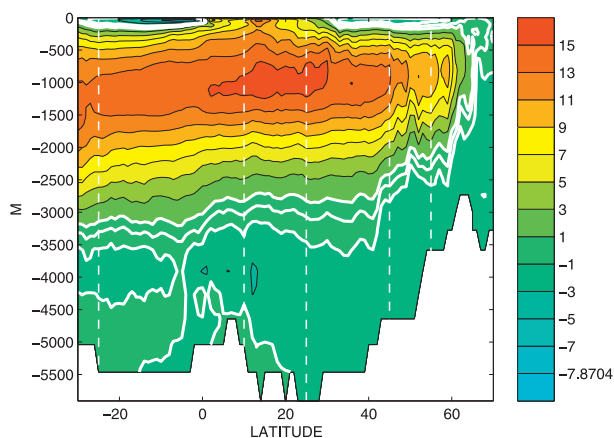


FIG. 2. Accumulating sum of V_{cc} (Sv) to the bottom showing the changing maximum depth and near zero at the bottom.

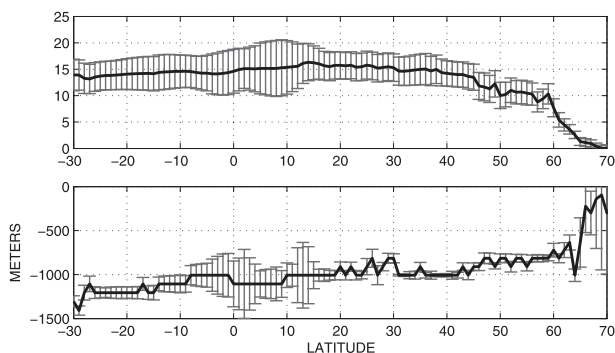


FIG. 3. (top) The V_{MOC} (Sv) as defined as the value maximizing meridional transport when integrated from the sea surface downward. Error bars are from the monthly standard deviation. (bottom) Integration depth maximizing northward transport (upper part of the panel) when integrated downward from the sea surface. Error bars are from the monthly standard deviation.

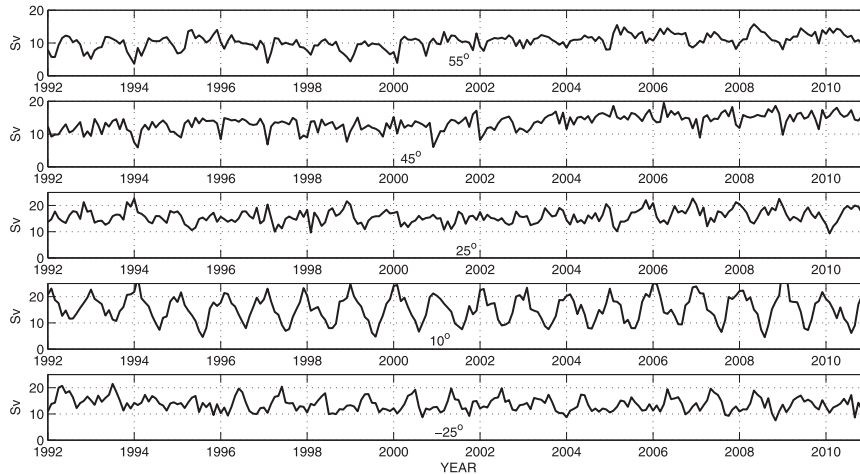


FIG. 4. Monthly values of the estimated MOC at five latitudes. Note differing scales. The 10°N values are dominated by the annual cycle.

maintained over essentially all periods shorter than about 42 months (3–4-yr period) when there is a shift to being in phase, although the coherent power at these longer periods is very small. Within the subpolar region, between 45° and 55°N , coherence at zero phase exists at periods beyond about 4 yr.

Removing all energy at periods shorter than 1 yr permits the display in Fig. 10 of the zero-time-lag meridional correlation structure of motions out to 19 yr (consistent with the zero phases seen in the coherence calculations at long periods). As in Wunsch (2012), essentially no interannual correlation in the variations exists across about 35°N latitude—variations in the subpolar and subtropical gyres being decoupled. Such

decoupling is also apparent between 55° and 65°N . A small region of apparently significant correlation does exist between the far South Atlantic and the subpolar regions (between 45° and 60°N) of the North Atlantic without an intermediate covarying structure. Two immediate possible explanations suggest themselves: 1) the correlation lies with corresponding covariations in the wind field between these latitudes. 2) An internally controlled oceanic transport correlation exists between intermediate latitudes but is lost in the noise of oceanic variability, which is highest in low latitudes and in the region of the eastward-moving Gulf Stream (Fig. 10). If the latter is the correct explanation, only many more years of data will begin to show the covariation. The

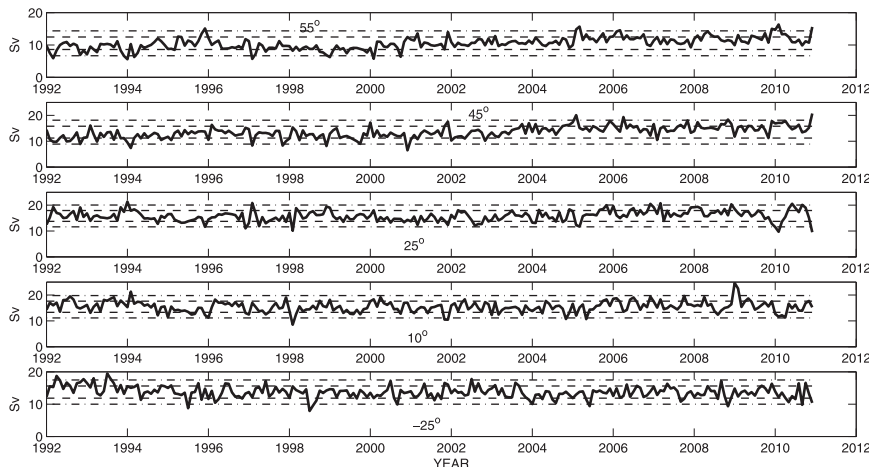


FIG. 5. AMOC with no deterministic annual cycle or overtones at five latitudes. Horizontal lines show the one and two standard deviation ranges about the 19-yr means. A weak visual trend of unknown significance is visible at 45° and 55°N . For white noise, approximately 5% of the values should be above or below the 2σ levels.

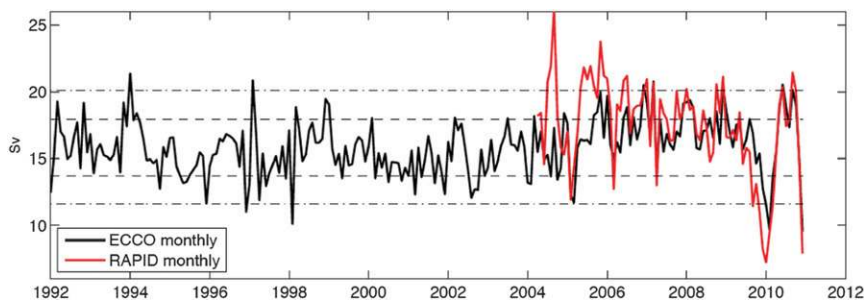


FIG. 6. The 25°N AMOC on an expanded scale as estimated by the ECCO–Production ver4 (black curve), thus dramatizing the variations seen in Fig. 5. Monthly values with the annual cycle and harmonics removed. The 1σ and 2σ levels are shown. The RAPID–Meridional Overturning Circulation and Heatflux Array (MOCHA) estimate available since 2004 is shown in red.

presence of a weak visual trend in high northern latitudes also does render the significance test as somewhat optimistic because the corresponding excess serial autocorrelation in V_{MOC} , reducing the degrees of freedom, has not been accounted for. In any case, a true correlation of 0.5

would imply that an upper bound of 25% of the variance in one latitude band could be calculated from knowledge of variations at the other. [See Bingham et al. (2007) for a pure model result that is very similar to the present one, as well as the recent review by Srokosz et al. (2012).]

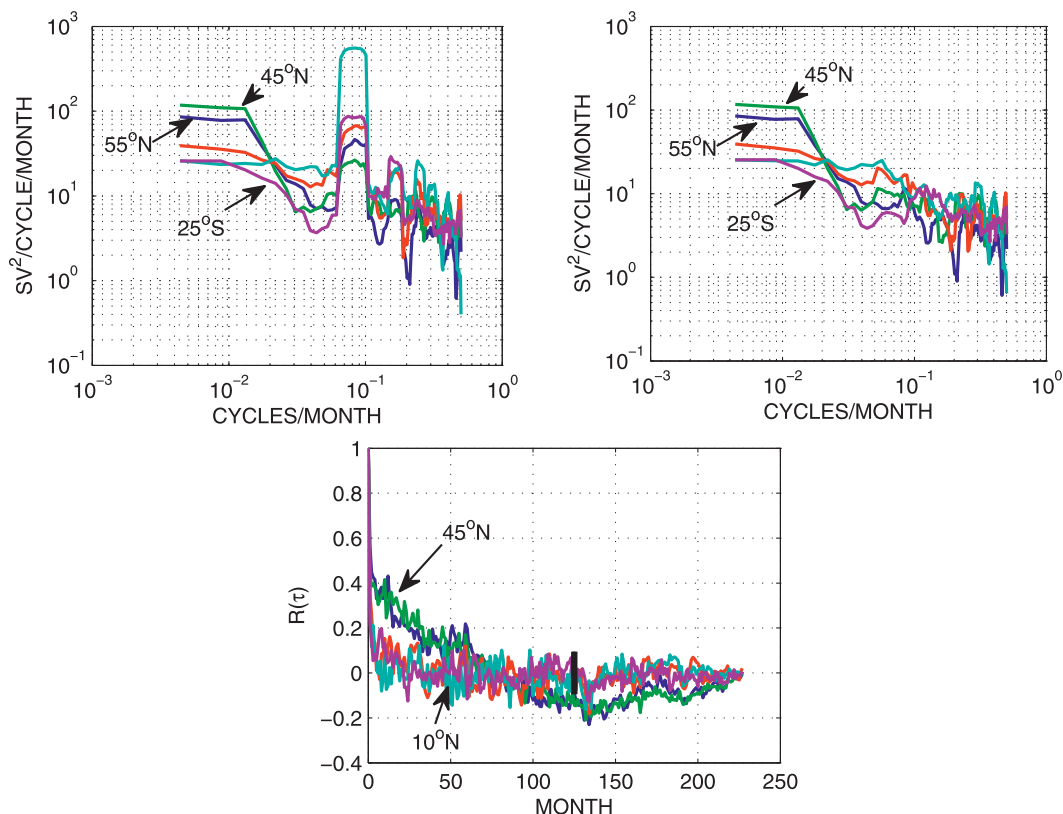


FIG. 7. Multitaper-method power spectra density estimates at five representative latitudes with the annual cycle and overtones (top left) present and (top right) removed. (bottom) The autocorrelation function corresponding to power densities in the top right panel. Apart from the annual cycle, the spectra at the lower three latitudes are weakly red and have a steeper slope at 45° and 55°N. The vertical line segment in the autocorrelation plot is the one standard deviation error bar using the Priestley [1981, his Eq. (5.3.41)] asymptotic estimate.

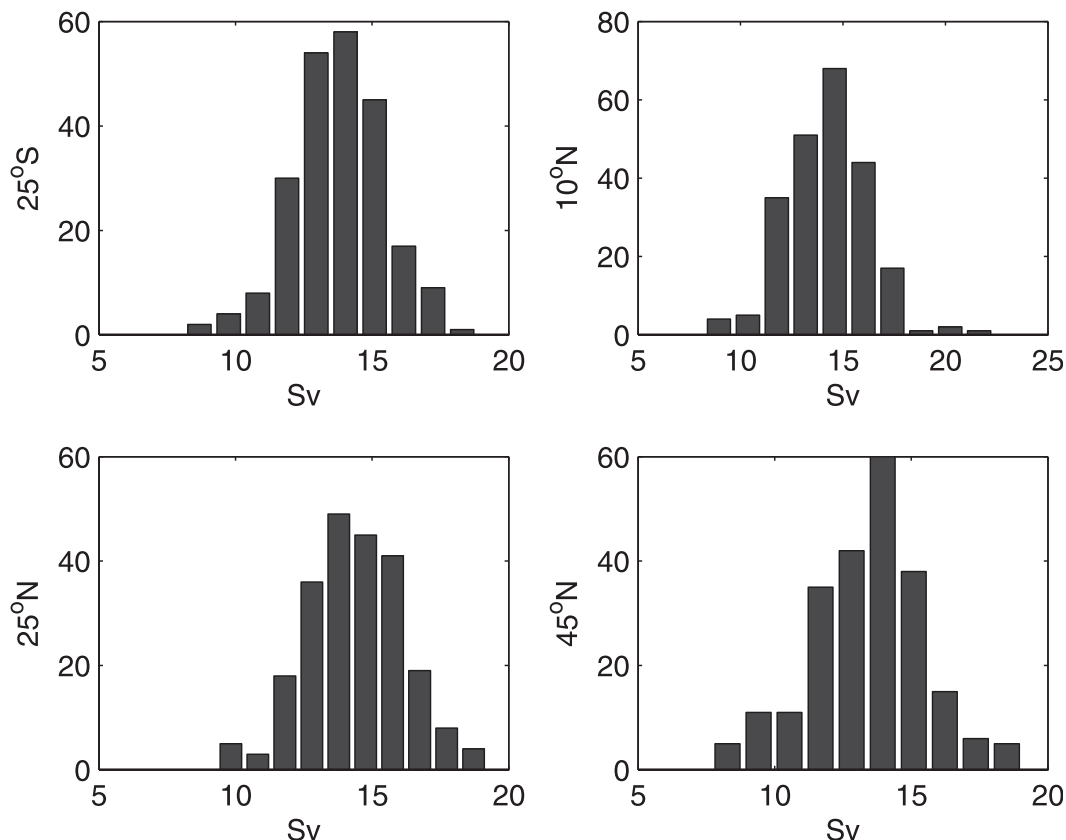


FIG. 8. Histograms of the AMOC monthly residuals (after removal of the annual cycle and its harmonics) for 25°S, 10°N, 25°N, and 45°N.

5. The structure

In the region where the Gulf Stream is confined between landmasses and called the Florida Current, many years of observations by many methods [see, e.g., Meinen et al. (2010)] have shown that its time-mean transport is approximately 31 Sv. The value of the AMOC then is the difference between the 31 Sv of the northbound Gulf Stream and whatever value is being returned above about 1000 m, leaving, roughly, 15–16 Sv. At this point, it is worth stopping and asking how that particular value arises.

A very large effort has gone into calculating this number in models, as discussed, for example, in the IPCC reports³ and from inferences about the past from proxy data [e.g., protactinium/thorium; see Peacock (2010); Burke et al. (2011)]. Why is it 15–20 Sv and not 5 or 50 Sv? For present purposes, we focus on the region at about 30°N. This position is just north of the double western boundary region, where the Gulf Stream is land confined and that current will have essentially the same

transport and properties as at 30°N but the latter usefully lacks the complication of having separate western margins for the interior flow and the western boundary current.

In the simplest of all equilibrium ocean current theories, dating back to the late 1940s, the northward flow in the boundary current would have all been sent southward again in the interior by the wind-driven Sverdrup-balance flow, confined to the upper ocean and overlying a quiescent layer. The result would be a vanishing AMOC. In their test of Sverdrup balance in the North Atlantic near this latitude, Leetmaa et al. (1977) indeed inferred that the entirety of the return flow took place above about 1000 m, apparently vindicating the theory. Wunsch and Roemmich (1985) noted, however, that if their inference was correct, the meridional heat transport in the North Atlantic would be considerably smaller than is believed plausible—because the upper layer brings warm water back south: in an oceanwide Sverdrup balance, the net temperature transport would be slight. Thus, all recent estimates of the oceanic meridional heat transport in the North Atlantic require failure of basinwide Sverdrup balance.

³ See, for example, Fig. 10.15 of Solomon et al. (2007).

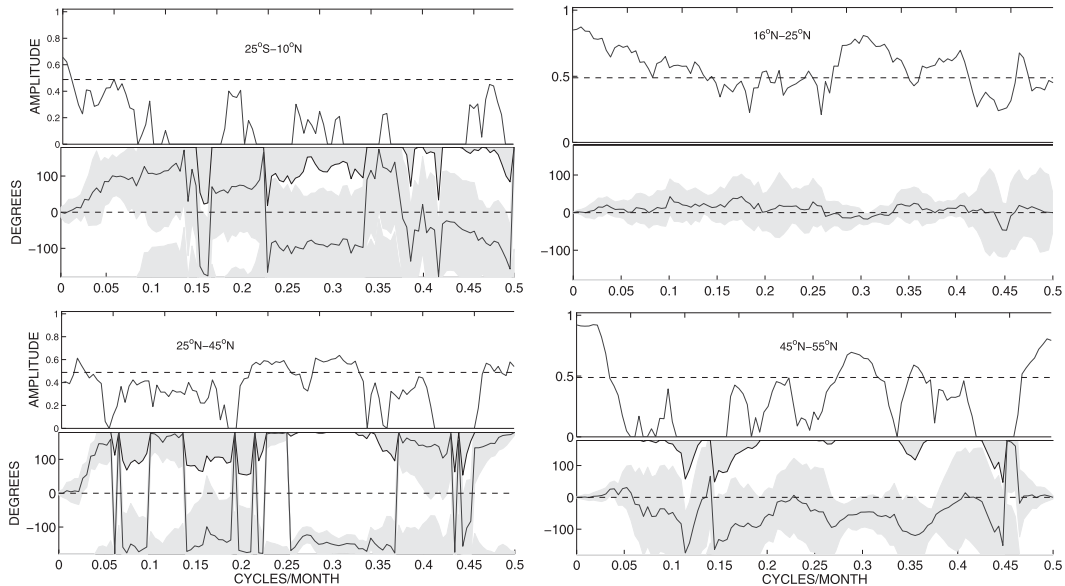


FIG. 9. Coherence magnitude and phase of the AMOC between four pairs of nearest-neighbor latitudes. The horizontal dashed line is an approximate level of no significance at 95% confidence and gray bands in phase show the approximate 95% confidence intervals. The 10° and 16° N pair is nearly redundant (not shown) having zero phase between about 19-yr and 3-month periods, with an avg amplitude of about 0.85. Except at the very longest periods estimated, no measureable coherence exists across the equator. Within the subtropical gyre, characterized by 16° and 25° N some coherence exists with phases indistinguishable from zero but with noticeably larger amplitudes at periods exceeding 1 yr and around 3 months. Slight coherence, at essentially 180° phase, exists across the Gulf Stream system (25° – 45° N) at periods of around 5–10 months, becoming zero phase at periods near to the 19-yr record length. Amplitudes are generally weak. Within the subpolar gyre, 45° – 55° N, significant coherence at zero phase exists at periods longer than about 3 yr.

Figure 11 shows that fraction of the North Atlantic where Sverdrup balance in a 16-yr average appears consistent with the observed flow [adapted from Wunsch (2011)]. Temperature transport numbers require it to fail at least in part and Fig. 11 shows where it appears to do so. The why of it (including the area covered), the depth to which one must integrate, the interdecadal variability, and the extent to which it is likely to change through time in the future are central to understanding the ocean circulation in climate. Note that its failure in the subpolar gyre is likely the result of having only 19 yr of data in a region where baroclinic adjustment times are on the order of 100 yr and longer (Wunsch 2011), and an equilibrium theory like this one would not be expected to be useful.

Figure 12 shows the 19-yr time-average meridional velocity across 30° N in the Atlantic. Various attempts to describe the structure in terms of vertically or horizontally integrated flows and their deviation exist (e.g., Kanzow et al. 2009). Unfortunately, the known physics show that the integrals lump together very different flow regimes. In moving away from the primarily description to questions of why the AMOC takes the values it does, a global breakdown into different dynamical regimes is required.

If one tries to pick apart the zonal structure of the subtropical North Atlantic Ocean, a long history of observation and theory suggests at least four major dynamical regimes exist, which can be qualitatively recognized in Fig. 12: 1) the western boundary current area, 2) the Gulf Stream recirculation (e.g., Schmitz and McCartney 1993), 3) a Sverdrup-like interior above an empirically determined depth z_S , and 4) the eastern boundary current region (Barton 1998). These subsets are themselves somewhat oversimplified as, for example, theory suggests an interesting dynamical regime inshore of the Gulf Stream where it rubs against the coast (Moore and Niiler 1974). Some of the literature speculates on the existence of an Antilles Current to the east of the Gulf Stream (e.g., Lee et al. 1996). Continental margins are the site of a complex amalgam of trapped motions, some quite slow because they involve diffusive processes. The eastern boundary current regime has a rich literature of its own and the surface mixed layer/Ekman flow exists but is here defined as part of the layer of Sverdrup balance—as Sverdrup himself considered it. For present purposes, the four regimes listed provide a useful, if crude, framework. In the vertical, one can think of a domain

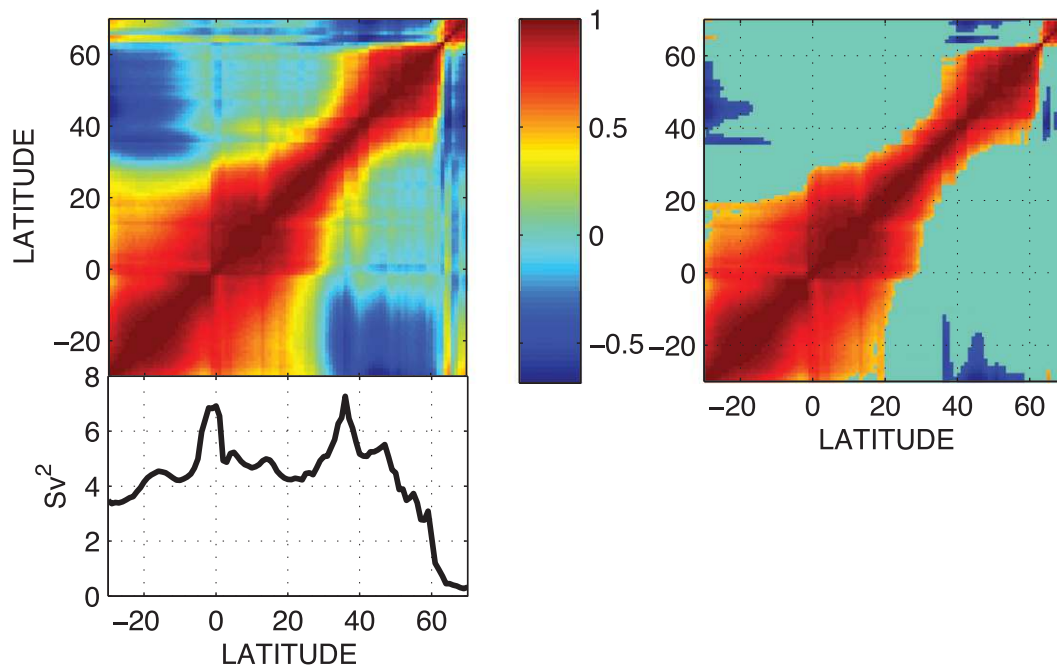


FIG. 10. Meridional correlation matrix of the AMOC for energy at periods longer than 1 yr and less than 19 yr but flipped to put the southernmost values in the lower left corner. The value along the main diagonal is necessarily 1. (left) The full matrix and (right) only values estimated as statistically nonzero at 95% confidence—nonsignificant values being set to zero. In contrast to the results in Wunsch (2012), one now sees a weak anticorrelation between the South Atlantic values and the high-latitude North Atlantic but no such correlation between low- and high-latitude North Atlantic variations. The AMOC variance, with a suppressed annual cycle, is shown in the lower panel, with considerable increases near the equator and across the Gulf Stream system, corresponding to positions with a loss of correlation.

that includes in (1) the deep western boundary current (DWBC) displaced by topography from the longitude of the Gulf Stream and in (3) the region below the Sverdrup integration depth z_S . Below that depth the southward meridional flow is generally associated with North Atlantic Deep Water (NADW) but it is interrupted by northward-going components. At this latitude, z_S lies between 1000 and 1500 m, somewhat noisily.

The recirculation regime appears to be quasi barotropic (Lee et al. 1996) and largely eddy dominated, but the extent to which that is true is left open here. Analysis of these regimes remains dynamically incomplete after 70 yr of effort, and we merely point out that questions such as what sets the approximately 15-Sv return flow above z_S and why z_S has the value it does as a function of position and averaging time raise many of the most fundamental open questions in physical oceanography.

These questions have been suppressed in much of climate modeling literature by the focus on a single AMOC number, although exceptions do exist. Observational discussions (e.g., of the observed RAPID results along 26°N) have started the process of describing the flow in terms of an interior, Ekman layer, western

boundary current transport, and so on (e.g., Srokosz et al. 2012). These, in turn, are coupled into the more distant ocean circulation and its variability. As long as the mass is nearly conserved, forced changes in abyssal total transports must be reflected in compensation in the upper ocean and vice versa, but the partitioning remains obscure and is surely a function of time scale. Heimbach et al. (2011) show that the North Atlantic Ocean circulation is sensitive to disturbances arising from the global ocean and occurs over time periods extending out to many decades, at least.

A further complicating factor in reducing the AMOC to one number is the Bering Strait throughflow from the Pacific Ocean across the Arctic Basin into the Atlantic on the order of 1 Sv as the mean (Woodgate et al. 2006; Aagaard et al. 1985) but with monthly values ranging from -1 up to $+3$ Sv; meaning that zonal and vertical transport integrals in the North Atlantic do not vanish. Interannual variations in their results are very large. Vertical integrals to the bottom from the present time-mean estimate are shown in Fig. 13 and would include the Bering Sea inflow plus whatever freshwater addition occurs within the Arctic and anywhere poleward of 70°N. The northernmost number shown is a reasonable

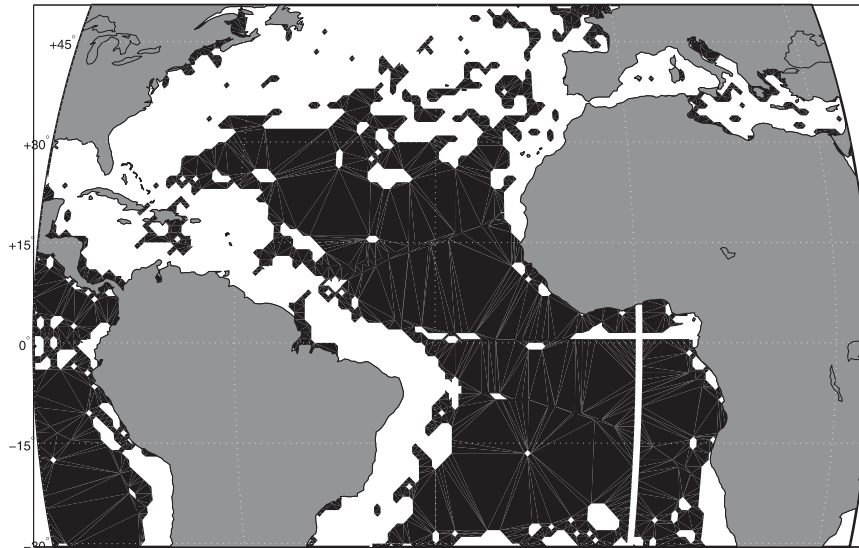


FIG. 11. Gray color depicts the region passing a test for pointwise applicability of Sverdrup balance [adapted from Wunsch (2011)]. The integration depth z_S is found empirically as the depth of minimum absolute vertical velocity and varies between 1000 and 2000 m in this region and is still noisy even with 16 yr of temporal and 5° of latitude–longitude spatial averaging. The meridional white band is the Greenwich meridian.

value of about 1.2 Sv to the south, and the general reduction by 30°S is consistent with the known behavior of the Atlantic as a net evaporative basin. A discussion of the structures superimposed is beyond the scope of this paper. Published estimates of the AMOC transport and its variations to fractions of a Sverdrup are difficult to interpret, if only because the vertical distributions of the net throughflow and of the precipitation, evaporation, and runoff disturbances are not known to those accuracies and are time dependent.

6. The AMOC as Gaussian red noise

As discussed above, with the available 228 monthly estimates, the AMOC variability at 25°N and other latitudes is indistinguishable from a stationary Gaussian red-noise process having a mean of 15.5 Sv and variance of $6.7\text{ Sv}^2 = (2.6\text{ Sv})^2$ of which 1.1 Sv^2 is contributed at periods longer than a year. This slight variation has multiple causes. The component of the return flow in Sverdrup balance is a direct reflection of the strength of

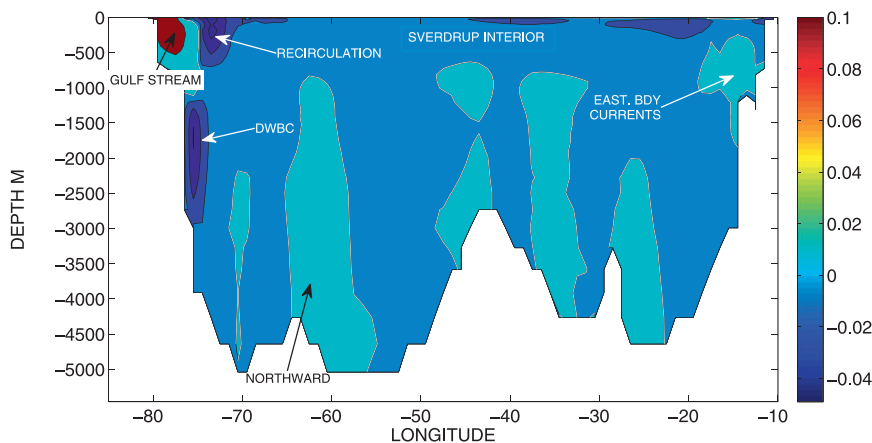


FIG. 12. Time-avg meridional velocity at 30°N from the 19-yr ECCO–Production version 4 estimate. A schematic of dynamical subdomains is overlaid. The Ekman layer is included in the Sverdrup-balance region and other subdomains such as that between the Gulf Stream and the western boundary have been omitted. In this region, the empirical Sverdrup balance integration depth z_S ranges between about 1000 and 1500 m. Longitudes are west values.

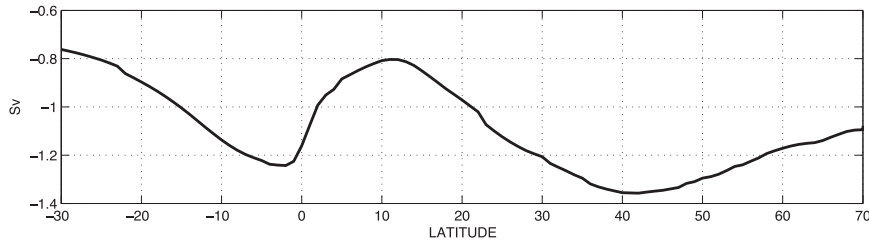


FIG. 13. Vertical integral of the time-mean zonally summed meridional flow. The nonzero values represent a combination of volume entering from the Arctic (Bering Strait in part) plus divergences and convergences of local precipitation minus evaporation.

the wind curl. A wind curl shift of about 7%, if sustained, produces approximately a 1-Sv change in that component. Such variations are seen all the time. (Wind field fluctuations are discussed specifically below.)

Similarly, suppose there is a 1-Sv increase (decrease) in the mass flux above 1000 m and sustained for 1 yr, then the excess (deficit) can appear as a shift in watermass volume. Assuming, for the sake of a scale, that the ocean accommodates this shift southward of about 40°N (very roughly the latitude of the Gulf Stream), then the relevant ocean area between 25° and 40°N is about 10^{13} m^2 . An isopycnal (absent mixing) would have to move by 3 m during the year—a storage change, in the presence of the eddy field and realistic sampling, well below any existing detection capability. Alternatively, storage changes of that magnitude, being released over time, would appear as transport fluctuations of the size observed.

None of the variations observed can be regarded as more than small perturbations upon the large-scale background ocean. The fragmentary historical record contains no indication of large-scale changes that would need to be regarded as demanding a conspicuously nonlinear response. Obviously nonlinear regions,

undergoing major change, exist in the convective and sea ice regions at high latitudes (e.g., Griffies and Bryan 1997), but these occupy a trivial fraction of the volume of the ocean, which appears to have remained essentially geostrophic and hydrostatic for at least hundreds of years. The careful documentation by Roemmich et al. (2012) of the shifts in upper-ocean temperature since the 1873–75 HMS *Challenger* expedition shows that they represent minor perturbations of the basic upper-ocean stratification. A transport estimate derived from the *Challenger* section across the Gulf Stream is entirely consistent with modern estimates (Rossby et al. 2010). Away from the equator, changes in the gross baroclinic structure of the oceans involve very slow processes.

Figure 14 displays the time-average (19 yr) absolute sea surface topography along with its standard deviation, and Fig. 15 shows its changes from year to year over the last 4 yr. The complex spatial variations have an amplitude of about 5 cm and correspond to transport disturbances of many tens of Sverdrups. That the AMOC appears to be dominantly a stochastic variable is to be expected: atmospheric forcing via wind, freshwater, and enthalpy exchange decorrelates rapidly in space and time on the synoptic scale (where most of the energy is,

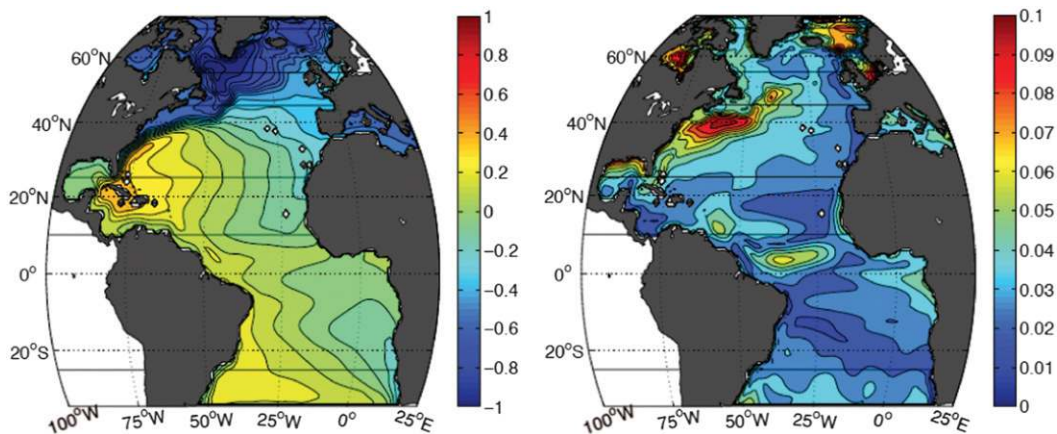


FIG. 14. Estimated 19-yr time-avg sea surface elev (m) relative to the (left) geoid and (right) corresponding standard deviation.

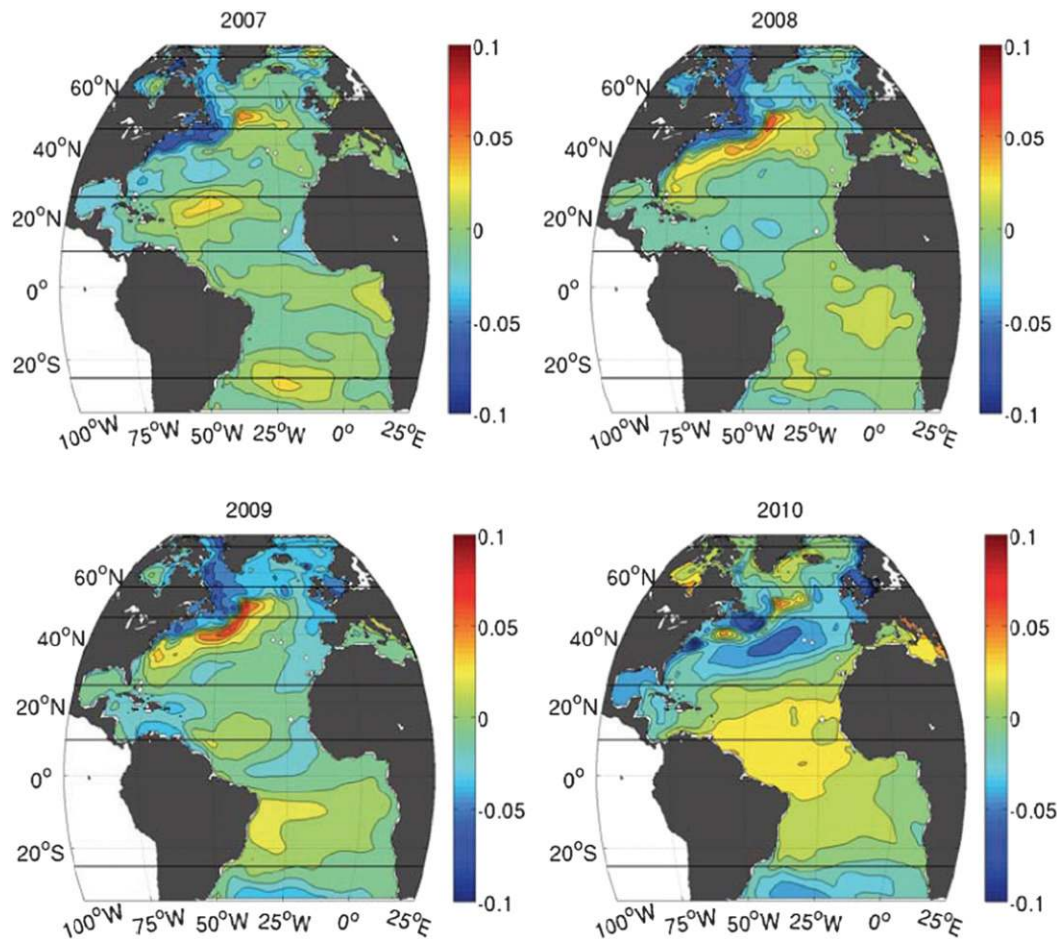


FIG. 15. Surface elev anomaly (m) for the last 4 yr (2001, 2008, 2009, and 2010) of the calculation. An elev change of 1 cm at midlatitudes with pressures extending to the bottom corresponds to approximately 7 Sv of transport.

and fluctuations such as the ones subsumed under the North Atlantic Oscillation (NAO) index have a temporal memory of barely 1 yr. Zero-order trends (relative to the time means) over decades have been difficult to perceive and are clearly small. The ocean integrates all of these disturbances, plus those arising from internal and forced instabilities of a great variety, over thousands of kilometers and thousands of years. These collective disturbances will appear in the AMOC at any given latitude. Because of absent major trends in the forcing functions, with those trends large enough to dominate the variability, a stochastic outcome is to be expected [cf. Chhak et al. (2006) for a pure modeling study of a response to stochastic forcing by wind alone and for further references].

No existing theory predicts the depth z_s to which the Sverdrup flow should extend. With other elements fixed, the strengthening of the Sverdrup transport, whether from a larger velocity or a more extensive volume over which it occurs, would weaken the AMOC. The deeper transports are a summation of deep western boundary

current strengths and volume fluxes emanating from both the south and north with, again, no theoretical foundation for quantitatively determining the changing net values. Mass being conserved and major sea level or isopycnal shifts not observed, volume fluxes above and below some empirical dividing depth will always nearly be balanced. Evidently, AMOC strength is a problematic measure of circulation intensity. That minor shifts (a few Sverdrups) appear from month to month and year to year is unsurprising given, for example, the fluctuations in surface topography. To the contrary, it would be more surprising if they did not appear.

a. The wind stress

The ocean responds rapidly and effectively to changes in wind stress on time scales ranging from the barotropic—which is almost instantaneous—through the baroclinic boundary and equatorial waves moving at rates from meters per second to long asymptotic time scales of centuries for high-latitude interior baroclinic

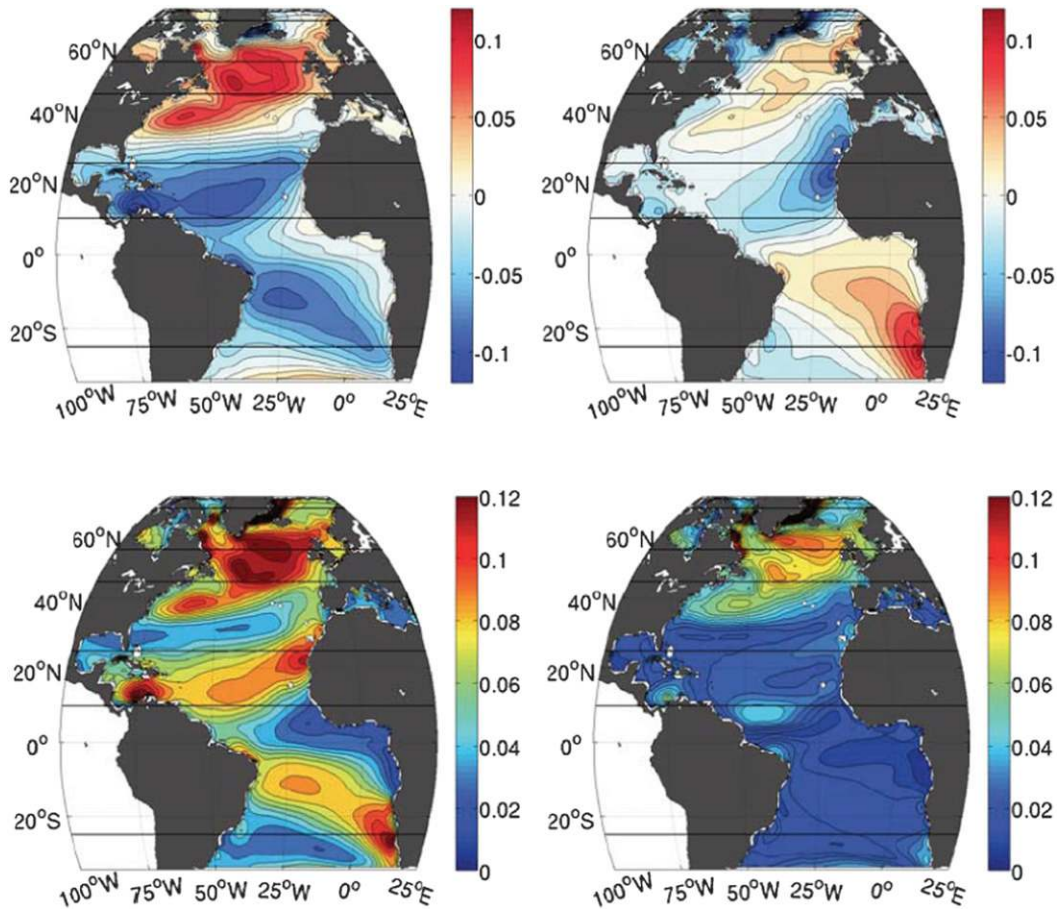


FIG. 16. Time-mean (top left) τ_x and (top right) τ_y (N m^{-2}). (bottom left) Time-mean $\|\tau\|$ and its (bottom right) standard deviation. The variations have the same order of magnitude as the mean.

adjustment. Within the system, the memory of past wind events must extend partially to decades and hundreds of years. With a 19-yr estimate it is hardly possible to explore all of these time scales, but one can, at a minimum, depict the magnitude of changes as seen over that interval and estimate fluctuations from year to year and longer out to a few years.

Figure 16 displays the time mean over 19 yr of the two components of wind stress τ and the resulting time-mean curl of the wind stress (Fig. 17). These are oceanographically unsurprising; apart, perhaps, from some of the small-scale structures that persist over 18 yr [see also Risien and Chelton (2008)]. Figure 17 is most relevant to the present discussion, displaying the difference between the 2010 annual-mean wind stress curl and that from 1994, normalized by the 19-yr time-mean curl. Evidently fluctuations in the curl regionally greatly exceed the time mean—by more than an order of magnitude at high northern latitudes. Even in the relatively quiet subtropical gyres, this difference is of the same order as the

mean itself. Large fluctuations in the AMOC at these latitudes are thus expected.

The noisiness of curl variability from year to year is confirmed by computing its singular vectors (empirical orthogonal functions; not shown). The full range of the 19 singular values is only about 0.3 from the largest to the smallest, and thus the patterns are not dominated by any simple large-scale changes.

b. Why is the variability nearly Gaussian?

Given the known nonlinearities of the ocean circulation, it may be surprising that the AMOC values are indistinguishable from a linear stochastic process. The explanation lies with the central limit theorem: the number of uncorrelated, and probably nearly independent, elements contributing to the values is so large that the sum becomes normally distributed. Fluctuations in the wind field are only a portion of the story, which includes buoyancy forcing, eddy noise, and so on.

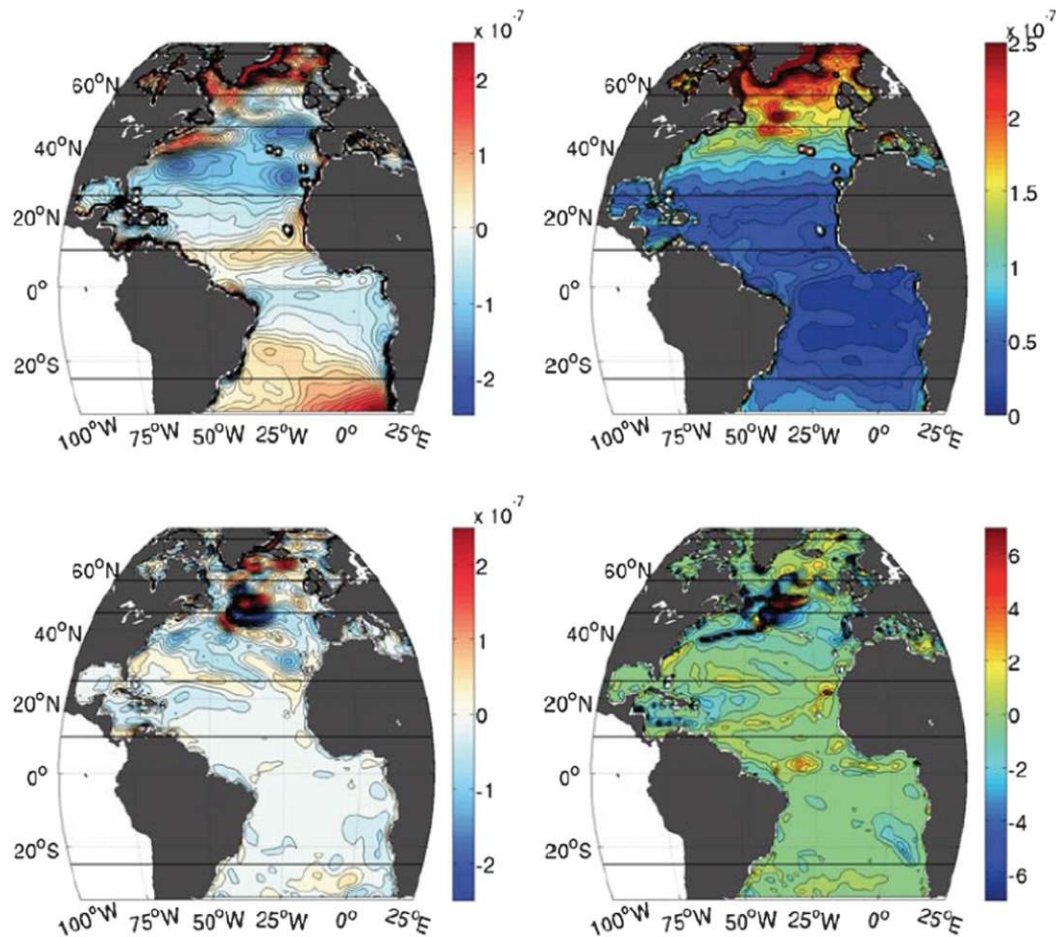


FIG. 17. (top left) Time-mean wind stress curl and (top right) standard deviation (N m^{-2}). (bottom left) The 1994 stress curl anomaly and (bottom right) the difference of the wind stress curl in years 2010 and 1994 normalized by $|\mathbf{V} \times \boldsymbol{\tau}| + 10^{-8}$. The value 10^{-8} was added to remove the singularity where the mean curl vanishes.

7. Trends, predictability, and extremes

a. Extreme events

Climate debates are commonly driven by observed extreme events and their interpretation. Plots of the AMOC values with a suppressed annual cycle (Figs. 5, 6) show that on a few occasions fluctuations exceed two standard deviations of the estimated mean values. An important question is whether those fluctuations (e.g., at 25°N in 1994 and 2010) are unexpected in records of this length. Under the assumption that one is dealing with stationary Gaussian processes with a known spectrum of variability, a well-understood theory (e.g., Vanmarcke 1983) permits estimates of the frequency of extreme events and their duration. Equation (4.4.5) in Vanmarcke (1983) produces an estimate that the rate of upward (or downward) crossing of the 2σ line should be roughly 0.06 month^{-1} so that in 228 months there should have been approximately 14 such excursions

upward (downward). The observed upward number is roughly 6, so one can infer that the number of extreme events is somewhat smaller than expected—the formula is, however, exponential in the estimated σ and involves other approximations. Note that the histograms in Fig. 8 lack long tails but are nonetheless, with this limited sampling, indistinguishable from the Gaussian processes.

An even simpler estimate can be made by noting that the 25°N AMOC is spectrally nearly white noise. A 2σ band is an approximate 95% confidence interval for a Gaussian process, and thus on this basis the AMOC at this latitude should be above or below the 2σ level of about $0.025 \times 228 = 6$ months of the time; this result is also difficult to distinguish from what is observed. These extreme events thus occur no more frequently than expected. Similar calculations can be made at the other latitudes but are omitted here on the basis that nothing unexpected in a stationary stochastic process has been seen.

b. Trend determination

The difficult problem of trend determination in climate records revolves around determining the low-frequency asymptote of the spectrum of natural variability, given that the oceans store disturbances from changes that occurred in the remote past. With the present estimates (Fig. 5), no visual evidence exists for a trend in the AMOC except in the subpolar latitudes of 45° and 55°N. These apparent trends are very weak and expected to be unstable as the record lengthens, as trends in the slowly adjusting model abyssal ocean begin to affect the upper layers, and as changes are made in model parameters. Indeed, subsequent state estimates with a slightly modified model show the fragility of these trends, and we attach no physical significance to them other than to observe their weakness relative to the underlying variability. If one optimistically assumes the covariances depicted in Fig. 7 are reasonable estimates of their true values, one can calculate the 95% confidence interval for a 20-yr trend in the AMOC in each place.

Under the Gaussian assumption, using the calculated temporal covariance at 25°N (not far from a delta function at the origin—consistent with white noise), one finds that a shift of 2 Sv over 19 yr would be statistically significant at 95% confidence. At 45°N, a change of about 4.5 Sv would be required for 95% significance, as a combination of the higher noise variance and the reduced number of independent measurements resulting from the longer time correlation. This latter calculation assumes that the visual trend is part of a red-noise background and is not itself a secular response of indefinite duration. It is not clear whether this hypothesis is correct, but it is consistent with known long adjustment times of high-latitude baroclinic oceans and does emphasize the need for a much better understanding of natural variability in the limit as the frequency approaches zero (which is an unreachable limit).

c. Prediction

The slightly reddish spectra show that the AMOC has a slight degree of predictability, discussed at greater length by Wunsch (2012), although the present longer duration results show a weaker serial correlation and thus less predictability than was found earlier. Pure white noise has no predictability beyond its mean value. To the extent that the estimates are indistinguishable from a linear system, analytical expressions are available for the prediction error as a function of time. Optimal linear prediction of stationary time series is, in essence, the study of the time-lagged memory in the process. One can distinguish monthly interval predictability from annual-average predictability.

Consider first the prediction of the 228-sample 25°N process, written as a predictive decomposition. Least squares fitting (e.g., Ljung 1999) produces the form

$$V_{\text{MOC}}(t, 25^\circ\text{N}) = m_v + \theta(t) + 0.30\theta(t - \Delta t) + 0.17\theta(t - 2\Delta t), \quad (4)$$

where $\theta(t)$ is zero-mean white noise with variance of about 3.7 Sv^2 , $\Delta t = 1$ month, and m_v is the sample time mean. Consistent with the slightly red spectrum, some prediction skill exists one month ahead, accounting for about 7% of the expected variance. [Coefficients in (4) have a calculated uncertainty, but it is not important here.]

If one uses the annual-average values (Fig. 6), the corresponding form is

$$\bar{V}_{\text{MOC}}(t, 25^\circ\text{N}) = m_v + \theta(t) + 0.88\theta(t - \Delta t), \quad (5)$$

where now $\Delta t = 1$ yr, and the variance of the (different) white-noise process is now approximately 0.7 Sv^2 . Recall that only 19 annual-average samples are available, but continuing the optimistic assumption of stable estimates, some predictability exists (1 yr in advance) for about 25% of the expected variance. There is essentially no prediction skill (beyond the mean value) 2 yr into the future. These prediction horizons are even more pessimistic than others have found [e.g., Zanna et al. (2012) for the MOC and sea surface temperature or Branstator and Teng (2010) for upper-ocean temperature].

Similar analyses can be applied at higher latitudes, where the more strongly red spectra do imply greater predictability. These results are not shown here, in part because of the difficulty of distinguishing the visible high-latitude trends as being either a deterministic one for which this approach is unsuitable (and something that is a reflection of a stochastic red-noise spectrum for which this approach is suitable) or, most likely, both phenomena are present.

The central result is that there is no evidence that the estimated AMOC is anything other than a statistically stationary linear process, and no indication appears of any dramatic changes either under way or likely to occur soon. An important corollary of the behavior of the AMOC as a linear stationary stochastic process is that the apparent predictability will vary from month to month and year to year through expected fluctuations in sample autocovariances. No change in the underlying physics is implied unless the excursions exceed the limits of probability.

8. The AMOC as a climate indicator

Returning now to the focus on the North Atlantic MOC as a climate indicator, the difficulty of interpretation is apparent. As already noted, stronger interior flows can produce a weakened AMOC and vice versa. Similarly, should the temperature of this returning flow increase (How does it change? What determines it?), the heat transport would diminish with the volume transport being unchanged. The persistence in the literature of the AMOC as a descriptor of ocean circulation is easy to understand: it provides a seemingly simple-to-interpret gross descriptive measure. But as has been seen, it can be quite misleading in its representativeness of the circulation as a whole [see the discussion of contradictory inferences about paleocirculation in Peacock (2010) or Burke et al. (2011)]. A number of authors (e.g., Dima and Lohmann 2010) assert a relationship between the AMOC and sea surface temperature anomalies. These relations are commonly based upon models. How the putative relationships operate, in view of the complexity of the AMOC structure and of the near-surface oceanic boundary layer, is not addressed. A reviewer has objected that we are overstating the role the AMOC has had in discussions in climate change; without indulging in an extended review, note only that although a very large literature exists on the pieces of the ocean circulation combining to form the net AMOC, the science component of the most recent IPCC report (Solomon et al. 2007) discusses the MOC in 225 places but fails to even mention the western boundary current or Sverdrup balance and so on.

The near linearity of the system is important. To our knowledge, no evidence exists from anywhere in the open ocean in the last decades and centuries of any disturbance that is more than a small perturbation on the background state (temperature or volume transport, salinity or potential vorticity, etc.). That is, apart from the very small volumes of high-latitude ocean, where sea ice physics and convective changes have occurred, open-ocean physics appear dynamically nearly linear—despite the turbulent interactions in a rich mesoscale and submesoscale eddy field. This inference, if correct, has important implications both for modeling circulation changes and for their prediction.

Surely there are very low-frequency trends in the system, including those induced by gross Holocene climate changes, plus those extending back to the end of the last deglaciation. But they are, at least for the time being, lost in the stochastic noise of the ocean circulation. If measured as time to equilibrium (Wunsch and Heimbach 2008), it is probably safe to assume that disturbances more than about 5000 yr in the past are no

longer generating significant oceanic changes but that anything more recent will have a remnant signature, whether detectable or not.

More generally, the volume flux is contained in a complex three-dimensional time-varying flow, partitioned among western boundary current areas, the deep western boundary current, Sverdrup-like interior, boundary-current recirculations, interior abyssal flows, and eastern boundary current regions all coupled through various conservation requirements. Absent any comprehensive understanding of controls on these components and their properties, such as temperature or carbon content, variations in the AMOC are not easily interpreted as a diagnostic of the ocean circulation or its climate impacts. Thus, a weaker AMOC during the Last Glacial Maximum, if real, might only reflect an expansion of the part of the upper ocean in Sverdrup balance with a concomitant change in the abyssal flow. Cause and effect are not understood. That a model of the modern ocean reproduces the observed AMOC value within error bars is a necessary, but insufficient, test of model skill. To progress, one needs to pick apart the different components of the flow on a global basis and come to understand how they vary and why they vary. It is time to move on:

Everything should be as simple as possible, but no simpler. (Usually attributed to A. Einstein, but apocryphal; <http://quoteinvestigator.com>.)

9. Final discussion

The zero-order result here is that a modern ocean–ice GCM, when least squares fit to the 2-decade-long global datasets available since 1992, produces a dynamically consistent estimate of the Atlantic MOC, one which is indistinguishable from a stationary Gaussian red-noise process. With the benefit of hindsight, the result is unsurprising: a system with long memory is subject to continuous small stochastic disturbances by external processes (winds, precipitation, etc.), which themselves are decorrelated in time and space, and to internal instabilities of a wide assortment. These processes integrate over both time and space to manifest themselves as components such as the AMOC (Hasselmann 1976). Fluctuations, extreme events, and so on are all expected and are seen to occur at rates consistent with those that can be calculated from the basic statistical properties.

Given the long time scales of ocean memory, however (e.g., Wunsch and Heimbach 2008), it is perhaps surprising that the frequency spectrum is not more red than is observed. That it is not far from white noise is probably best ascribed to the AMOC dominance by the

upper ocean and barotropic wind-driven circulation from the top to bottom—circulations that, through Ekman pumping and continental margin controlled processes, respond comparatively rapidly. The result is thus dominated by the known white-noise behavior of the wind field and is then only slightly reddened by the longer oceanic time scales reflected in measurements of only 19-yr duration. The absence of important basin-scale sea level trends implies mass conservation is a controlling constraint, demanding that different parts of the system, laterally and vertically, compensate rapidly.

Published IPCC model estimates of the AMOC have a very wide range. A reasonable inference is that the diverse dynamical subcomponents making up this integral are even more divergent among the models. Understanding of oceanic variability cannot be determined from the AMOC alone and the global three-dimensional ocean circulation must be described with all of its space and time structure. Evidently, the requirements on future observational systems, both for direct use and for the testing of evermore complex numerical models, are far greater than what is now available.

We draw no inferences, beyond some minor speculation, about the behavior of the North Atlantic circulation in general, and the AMOC in particular, on time scales exceeding those of our database. In particular, the weak estimated trends at some latitudes are not regarded as physically significant beyond the fact of their weakness relative to the overall variability. Some model studies are suggestive of interesting covariances between, for example, sea surface temperature and the integrated AMOC properties occurring over many decades and centuries. The testing of such inferences against adequate databases is a problem left for other times and places.

Acknowledgments. This research is supported in part by NASA and NOAA through AMOC and ECCO grants and prepared while one of us (CW) was the George Eastman Visiting Professor at Balliol College and in Atmospheres, Oceans, and Planetary Physics, Oxford University. We had useful comments from O. Marchal, S. M. Griffies, J. Hirschi, an unhappy anonymous reviewer, and the editor A. Gnanadesikan.

REFERENCES

- Aagaard, K., A. T. Roach, and J. D. Schumacher, 1985: On the wind-driven variability of the flow through Bering Strait. *J. Geophys. Res.*, **90**, 7213–7221.
- Adcroft, A., and J.-M. Campin, 2004: Rescaled height coordinates for accurate representation of free-surface flows in ocean circulation models. *Ocean Modell.*, **7**, 269–284.
- , C. Hill, and J. Marshall, 1997: The representation of topography by shaved cells in a height coordinate model. *Mon. Wea. Rev.*, **125**, 2293–2315.
- , —, J.-M. Campin, J. Marshall, and P. Heimbach, 2004: Overview of the formulation and numerics of the MIT GCM. *Proc. ECMWF Seminar Series on Numerical Methods: Recent Developments in Numerical Methods for Atmosphere and Ocean Modelling*, Reading, United Kingdom, ECMWF, 139–149.
- Baehr, J., 2010: Influence of the 26°N RAPID–MOCHA array and Florida Current cable observations on the ECCO–GODAE state estimate. *J. Phys. Oceanogr.*, **40**, 865–879.
- Barton, E. D., 1998: Eastern boundary of the North Atlantic: Northwest Africa and Iberia. Coastal segment (18, E). *The Sea*, A. R. Robinson and K. H. Brink, Eds., *Regional Studies and Syntheses*, Vol. 11, John Wiley and Sons, 633–657.
- Bingham, R. J., C. W. Hughes, V. Roussenov, and R. G. Williams, 2007: Meridional coherence of the North Atlantic meridional overturning circulation. *Geophys. Res. Lett.*, **34**, L23606, doi:10.1029/2007gl031731.
- Branstator, G., and H. Teng, 2010: Two limits of initial-value decadal predictability in a CGCM. *J. Climate*, **23**, 6292–6311.
- Burke, A., O. Marchal, L. I. Bradtmiller, J. F. McManus, and R. François, 2011: Application of an inverse method to interpret $^{231}\text{Pa}/^{230}\text{Th}$ observations from marine sediments. *Paleoceanography*, **26**, PA1212, doi:10.1029/2010PA002022.
- Campin, J.-M., A. Adcroft, C. Hill, and J. Marshall, 2004: Conservation of properties in a free surface model. *Ocean Modell.*, **6**, 221–244.
- Chhak, K. C., A. M. Moore, R. F. Milliff, G. Branstator, W. R. Holland, and M. Fisher, 2006: Stochastic forcing of the North Atlantic wind-driven ocean circulation. Part I: A diagnostic analysis of the ocean response to stochastic forcing. *J. Phys. Oceanogr.*, **36**, 300–315.
- Dee, D. P., and Coauthors, 2011: The ERA-Interim reanalysis: Configuration and performance of the data assimilation system. *Quart. J. Roy. Meteor. Soc.*, **137**, 553–597.
- Dima, M., and G. Lohmann, 2010: Evidence for two distinct modes of large-scale ocean circulation changes over the last century. *J. Climate*, **23**, 5–16.
- Forget, G., 2010: Mapping ocean observations in a dynamical framework: A 2004–06 ocean atlas. *J. Phys. Oceanogr.*, **40**, 1201–1221.
- Gaspar, P., Y. Gregoris, and J. M. Lefevre, 1990: A simple eddy kinetic energy model for simulations of the oceanic vertical mixing: Tests at station Papa and long-term upper ocean study site. *J. Geophys. Res.*, **95** (C9), 16 179–16 193.
- Gent, P. R., and J. C. McWilliams, 1990: Isopycnal mixing in ocean circulation models. *J. Phys. Oceanogr.*, **20**, 150–155.
- Gilbert, J. C., and C. Lemaréchal, 1989: Some numerical experiments with variable-storage quasi-Newton algorithms. *Math. Program.*, **45**, 407–435.
- Griffies, S. M., and K. Bryan, 1997: A predictability study of simulated North Atlantic multidecadal variability. *Climate Dyn.*, **13**, 459–487.
- Hasselmann, K., 1976: Stochastic climate models. Part I: Theory. *Tellus*, **28**, 289–305.
- Heimbach, P., D. Menemenlis, M. Losch, J. M. Campin, and C. Hill, 2010: On the formulation of sea-ice models. Part 2: Lessons from multi-year adjoint sea ice export sensitivities through the Canadian Arctic Archipelago. *Ocean Modell.*, **33**, 145–158, doi:10.1016/j.ocemod.2010.02.002.

- , C. Wunsch, R. M. Ponte, G. Forget, C. Hill, and J. Utke, 2011: Timescales and regions of the sensitivity of Atlantic meridional volume and heat transport magnitudes: Toward observing system design. *Deep-Sea Res. II*, **58**, 1858–1879.
- Jayne, S. R., and J. Marotzke, 2001: The dynamics of ocean heat transport variability. *Rev. Geophys.*, **39**, 385–411.
- Kanzow, T., U. Send, and M. McCartney, 2008: On the variability of the deep meridional transports in the tropical North Atlantic. *Deep-Sea Res. I*, **55**, 1601–1623.
- , H. L. Johnson, D. P. Marshall, S. A. Cunningham, J. J.-M. Hirschi, A. Mujahid, H. L. Bryden, and W. E. Johns, 2009: Basinwide integrated volume transports in an eddy-filled ocean. *J. Phys. Oceanogr.*, **39**, 3091–3110.
- Lee, T. N., W. E. Johns, R. J. Zantopp, and E. R. Fillenbaum, 1996: Moored observations of western boundary current variability and thermohaline circulation at 26.5° in the subtropical North Atlantic. *J. Phys. Oceanogr.*, **26**, 962–983.
- Leetmaa, A., P. Niiler, and H. Stommel, 1977: Does the Sverdrup relation account for the mid-Atlantic circulation? *J. Mar. Res.*, **35**, 1–10.
- Ljung, L., 1999: *System Identification: Theory for the User*. 2nd ed. Prentice-Hall, 519 pp.
- Losch, M., D. Menemenlis, J. M. Campin, P. Heimbach, and C. Hill, 2010: On the formulation of sea-ice models. Part 1: Effects of different solver implementations and parameterizations. *Ocean Modell.*, **33**, 129–144, doi:10.1016/j.ocemod.2009.12.008.
- Lozier, S., 2012: Overturning in the North Atlantic. *Annu. Rev. Mar. Sci.*, **4**, 291–315, doi:10.1146/annurev-marine-120710-100740.
- McCarthy, G., and Coauthors, 2012: Observed interannual variability of the Atlantic meridional overturning circulation at 26.5°N. *Geophys. Res. Lett.*, **39**, L19609, doi:10.1029/2012GL052933.
- Meinen, C. S., M. O. Baringer, and R. F. Garcia, 2010: Florida Current transport variability: An analysis of annual and longer-period signals. *Deep-Sea Res.*, **57**, 835–846.
- Menemenlis, D., and Coauthors, 2005: NASA supercomputer improves prospects for ocean climate research. *Eos, Trans. Amer. Geophys. Union*, **86**, 95–96.
- Moore, D., and P. Niiler, 1974: A two-layer model for the separation of inertial boundary currents. *J. Mar. Res.*, **32**, 457–484.
- Peacock, S., 2010: Comment on “Glacial-interglacial circulation changes inferred from ²³¹Pa/²³⁰Th sedimentary record in the North Atlantic region” by J.-M. Gherardi et al. *Paleoceanography*, **25**, PA2206, doi:10.1029/2009pa001835.
- Petoukhov, V. K., A. Ganopolski, V. Brovkin, M. Claussen, A. Eliseev, C. Kubatzki, and S. Rahmstorf, 2000: CLIMBER-2: A climate system model of intermediate complexity. Part I: Model description and performance for present climate. *Climate Dyn.*, **16**, 1–17.
- Priestley, M. B., 1981: *Spectral Analysis and Time Series*. Academic Press, 890 pp.
- Rayner, D., and Coauthors, 2011: Monitoring the Atlantic meridional overturning circulation. *Deep-Sea Res. II*, **58**, 1744–1753.
- Redi, M. H., 1982: Oceanic isopycnal mixing by coordinate rotation. *J. Phys. Oceanogr.*, **12**, 1154–1158.
- Risien, C. M., and D. B. Chelton, 2008: A global climatology of surface wind and wind stress fields from eight years of QuikSCAT scatterometer data. *J. Phys. Oceanogr.*, **38**, 2379–2413.
- Roemmich, D., W. J. Gould, and J. Gilson, 2012: 135 years of global ocean warming between the *Challenger* expedition and the Argo programme. *Nat. Climate Change*, **2**, 425–428, doi:10.1038/nclimate1461.
- Rosby, T., C. Flagg, and K. Donohue, 2010: On the variability of Gulf Stream transport from seasonal to decadal timescales. *J. Mar. Res.*, **68**, 503–522.
- Schmitz, W. J., Jr., and M. S. McCartney, 1993: On the North Atlantic circulation. *Rev. Geophys.*, **31**, 29–49.
- Send, U., M. Lankhorst, and T. Kanzow, 2011: Observation of decadal change in the Atlantic meridional overturning circulation using 10 years of continuous transport data. *Geophys. Res. Lett.*, **38**, L24606, doi:10.1029/2011GL049801.
- Smith, W. H. F., and D. T. Sandwell, 1997: Global sea floor topography from satellite altimetry and ship depth soundings. *Science*, **277**, 1956–1962.
- Solomon, S., D. Qin, M. Manning, Z. Chen, M. Marquis, K. Averyt, M. B. Tignor, and H. L. Miller Jr., Eds., 2007: *Climate Change 2007: The Physical Science Basis*. Cambridge University Press, 996 pp.
- Srokosz, M., M. Baringer, H. Bryden, S. Cunningham, T. Delworth, S. Lozier, J. Marotzke, and R. Sutton, 2012: Past, present, and future changes in the Atlantic meridional overturning circulation. *Bull. Amer. Meteor. Soc.*, **93**, 1663–1676.
- Vanmarcke, E., 1983: *Random Fields: Analysis and Synthesis*. MIT Press, 382 pp.
- Woodgate, R. A., K. Aagaard, and T. J. Weingartner, 2006: Interannual changes in the Bering Strait fluxes of volume, heat and freshwater between 1991 and 2004. *Geophys. Res. Lett.*, **33**, L15609, doi:10.1029/2006GL026931.
- Wright, D. G., and T. F. Stocker, 1991: A zonally averaged ocean model for the thermohaline circulation. Part I: Model development and flow dynamics. *J. Phys. Oceanogr.*, **21**, 1713–1724.
- Wunsch, C., 2011: The decadal mean ocean circulation and Sverdrup balance. *J. Mar. Res.*, **69**, 417–434.
- , 2012: Covariances and linear predictability of the Atlantic Ocean. *Deep-Sea Res. II*, **85**, 228–243, doi:10.1016/j.dsr2.2012.07.015.
- , and D. Roemmich, 1985: Is the North Atlantic in Sverdrup balance? *J. Phys. Oceanogr.*, **15**, 1876–1880.
- , and P. Heimbach, 2007: Practical global oceanic state estimation. *Physica D*, **230**, 197–208.
- , and —, 2008: How long to ocean tracer and proxy equilibrium? *Quat. Sci. Rev.*, **27**, 1639–1653, doi:10.1016/j.quascirev.2008.01.006.
- , and —, 2013: Dynamically and kinematically consistent global ocean circulation and ice state estimates. *Ocean Circulation and Climate*, 2nd ed. G. Siedler et al., Eds., Elsevier, in press. [Available online at http://ocean.mit.edu/~cwunsch/papersonline/state_estimates_22sep2012.pdf.]
- Zanna, L., P. Heimbach, A. M. Moore, and E. Tziperman, 2012: Upper-ocean singular vectors of the North Atlantic climate with implications for linear predictability and variability. *Quart. J. Roy. Meteor. Soc.*, **138**, 500–513, doi:10.1002/qj.937.